DESIGN OF A HOT PLUME INTERACTION FACILITY AT DLR COLOGNE

Dominik Saile[1], Daniel Kirchheck[1], Ali Gülhan[1], and Daniel Banuti[2]

[1]*DLR, German Aerospace Center, Institute of Aerodynamics and Flow Technology, 51147 Cologne, Germany*
[2]*DLR, German Aerospace Center, Institute of Aerodynamics and Flow Technology, Spacecraft, 37073 Göttingen, Germany*

ABSTRACT

Space transportation systems are exposed to high thermal and mechanical loads during the ascend in the transonic flow regime. By now, there are still many uncertainties, which can not be solved with state of the art computational fluid dynamic models or experiments with cold jet flows. A test facility with a high degree of similarity to flight with respect to the influence of the hot nozzle flow can contribute to improve the understanding of interaction effects between the hot nozzle flow and the ambient flow by providing reliable data for validation. The objective of the paper at hand is to present the work progress on such a facility. Issues and challenges concerning the base flows are discussed and potential research areas for investigations are considered. Relevant conditions during the ascend of *Ariane 5* are used as baseline and appropriate scaling laws are discussed to conclude requirements for the operational conditions for the existing wind tunnel *Vertical Test Section Cologne* (VMK). These operational conditions are used to develop a concept. After a proof of concept is given by CFD calculations, details to the supply system including the operational range are described and opposed to existing test benches without interaction capabilities.

Key words: LaTeX; Space transportation system; hot plume interaction; GOX/GH2; transonic flow regime; base flow;.

1. INTRODUCTION

At $T + 137\,\mathrm{s}$ into the flight 157 of *Ariane 5 ECA*, a pressure drop at the dump cooling outlet appeared, which is characteristic for a leak in the cooling system of the *Vulcain 2* rocket engine. In the following, a rapid degradation of the cooling of the nozzle was observed, which led to a loss of the nozzle's integrity and finally to a loss of control over the launcher's trajectory. This is what was presented in Paris by the inquiry board in the press conference with respect to this failure [1, 2]. The non-exhaustive definition of the design loads, combined with a combination of various stress factors during flight was declared to be on one of the most probable cause for the failure.

The objective of the paper at hand is to describe the ongoing efforts at the DLR Cologne to upgrade the *Vertical Test Section Cologne* (VMK) [3, 4] to enable the investigation of the hot flow interaction phenomena. In detail: The interaction of a hot exhaust jet with the ambient flow is of interest. For this reason, VMK must be equipped with a supply facility of gaseous oxygen and gaseous hydrogen. In this paper, concept is developed and a proof-of-concept of the some aspects of the scaling issue is conducted by means of numerical simulations. The concept includes the test environment like the wind tunnel itself, the model, the supply system and the measurement equipment.

In the long-term, the objective is to provide a platform in a field where CFD is not available yet or difficult/costly to obtain, and thus data for validation is required. The facility will allow the investigation of isolated flow effects like for cold flow jets and combined flow effects with chemical reactions, radiation, particles of various mass and size, condensation, high temperature or viscosity effects over a wide Mach number range with appropriate measurement techniques with a state of the art spatial/temporal resolution for propellants being identical to current space transportation systems or reflecting certain desired properties. This way, the hot plume testing facility will help to rule out discrepancies and inconsistencies between in-flight measurements, wind tunnel measurements and CFD and improve the understanding of the flow phenomena of rockets.

The paper is structured as follows: In the next section, a strong justification is given for such a facility by discussing the underlying motivation, which is a based on a short discussion of the numerous issues during the ascend of a space transportation system. This is the field of future measurements and applications. Additionally, some kind of inventory is given with respect to state-of-the-art developments in the space transportation field, considerations to scaling issues and the available test environment and equipment. The next section deals with the methods, and lists how the scaling laws are applied to find the operating range of the facility, details to the numerical

simulation, and input parameters to enable a selection of suitable measurement techniques.

2. MOTIVATION, APPLICATIONS, JUSTIFICATION AND INVENTORY

2.1. Exhaust Plume Induced Challenges on Space Transportation Systems

The catastrophic event from the introduction is continued here to elaborate some more details to the loads that space transportation systems are exposed. The first note of an abnormality of *Ariane 5* operation was $T + 137\,\mathrm{s}$ at the booster separation, which takes place at an altitude of about $68\,\mathrm{km}$ [5, 6] with about $2000\,\mathrm{ms}^{-1}$. Despite this high altitude, it is commonly accepted that the most challenging environment wrt to mechanical loads is during the transonic flight phase. For instance in Ref. [5], it can be seen that the highest dynamic pressure is reached at an altitude of $6.8\,\mathrm{km}$ and a velocity of $487.7\,\mathrm{ms}^{-1}$, which corresponds to Mach 1.56. Ref. [7] presents flight data and wind tunnel tests regarding the buffet loads on the *Ariane 5* afterbody. It can be seen that the unsteady loads on the nozzle like the pressure fluctuations, vibrations and actuator loads are strongest in the transonic flight regime and decrease over the flight time and corresponding higher Mach numbers ($Ma > 1.5$). This statement is supported in Ref. [8]. The article reports of flight data that reveal anomalous side loads acting on the *Vulcain 1* nozzle, which where then investigated experimentally [9] and numerically [10] on tolerable loads. ESA described the magnitude of the buffet loads as a major concern [11]. It is attributed to disturbances induced by the three-dimensional flow and the interaction with the boosters and started a series of activities concerning a possible coupling between the external flow and the shock-separated flow in the nozzle.

In general, buffeting describes the response of structural modes to aerodynamic/buffet loads. The relevance of axis-symmetrically excited loads was pointed out by Fuchs et al. [12] since they contribute significantly to the lateral force in the base region. Further, H. Wong [13] indicates that base-flow buffeting may trigger three-dimensional flow separation, and thus side loads during flight, which poses a serious issue for rocket nozzles [14].

As basis for the further descriptions and discussions, the mean flow topology of the near field at the generic base of an axis-symmetric generic rocket base is shown in Fig. 1. For the flow topology and the following considerations of the paper at hand, *Ariane 5* is used as reference with respect to the physical properties and generic, geometric dimensions.
The flow topology sketch is based on numerical simulations at Mach 0.7 conducted by Deck and Thorigny [15]. The sketch shows the incoming ambient flow along the vehicle (1) with the subsequent separation of the flow at the end of the main body (2). The flow is deflected to-

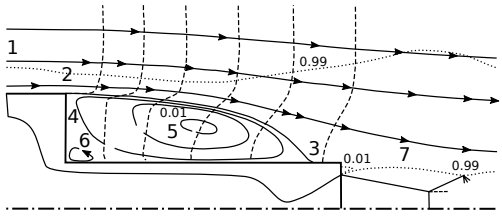

Figure 1. Near field flow topology at the base for an overexpanded nozzle flow in a subsonic external flow (sketched from Ref. [15]).

wards the nozzle and reattaches - depending on the ambient conditions, which is mainly the Mach number - on the nozzle (3) or on the supersonic jet acting as fluidic wall. The ambient flow and the vehicle/model walls enclose a highly energetic and unsteady recirculation region (4). In a time-averaged consideration, the flow features a large primary vortex (5) and a secondary corner vortex (6). The transonic flight phase is reached at a very early stage during the ascent (see e.g. Ref. [5]), thus the nozzle flow (7) - at least for the *Vulcain 2* engine with a very high expansion ratio - is overexpanded (Ref. [16]). The supersonic jet is predominantly inviscid and turbulent mixing processes takes place at a confined shear layer (7) to the ambient flow. The isolines marked with 0.01 and 0.99 depict the correspondent local velocity with normalized with the ambient flow. Additionally, the velocity profiles in the recirculation region are plotted at different distances downstream from the separation. Note that the instantaneous flow fields do not resemble the averaged flow field and is highly turbulent.

The emanating shear layer from the edge of the main body is assumed to be the driving force for the buffeting instability. Kelvin-Helmholtz form at the shear layer interface between the recirculation region, travel downstream and impinge on the *Vulcain* engine nozzle. According to the hypothesis of Wong et al. [8], this results in acoustic waves generated at the reattachment location, which travel upstream and may couple with the separation from the shoulder. In resonance, the effect may lead to an amplification of the amplitudes in the shear layer excitation. Via this feed-back loop, energy might be fed into recirculation region.
This aero-acoustic feedback loop hypothesis was reviewed by Deck and Thorigny [15]. His investigations reveal that the axis-symmetric separating/reattaching flow is governed by large scale coherent motions. According to experiments run by Deprés [17], more than 90% of the pressure fluctuations can be attributed to the antisymmetric mode $m = 1$, which is associated with helical vortex structures randomly orientated in the azimuthal direction as described by Fuchs et al. [12] for a flow past a circular disk. Further, it is stated by Deck and Thorigny [15] that shear layer *flapping* and shear layer *shedding* are different aspects of the same motion. The first describes a periodic growth and decay process of the recirculation bubble in the vertical direction with a characteristic fre-

quency of $fL_r/U\infty \approx 0.08$ (based on the reattachment length L_r). Further, Ref. [15] finds the secondary corner vortex growing and decaying with the same frequency. Shear layer shedding and the movement of the reattachment length are associated with $fL_r/U\infty \approx 0.2$. According to experiments mentioned in Ref. [15], 50% of the pressure fluctuations are attributed to this characteristic frequency. The onset for such a coherent large scale motion results from a feedback process between the separation point and the maximum intensity backflow location of the recirculation region, which is found to be origin of the absolutely unstable flow region. The generation of pressure waves is attributed to an interaction between the passage of large-scale and free-stream inrush between vortices. Recently, Weiss et al. [18] confirmed the hypothesis of an absolute unstable flow region by means of linear stability analysis coupled with a two-point correlation analysis.

Unsteady loads are only one reason for the justification of a hot plume testing facility. Ref. [19] lists many applications where an improved knowledge about rocket exhaust plumes is of interest like for the (1) design, the development and the operation of flight vehicles, to (2) detect and track flight vehicles, to (3) minimize radio-frequency interference and to (4) develop generally a better understanding for the plume behavior to provide foundations for simulations, to optimize intrinsic features wrt radio frequency attenuation, noise et cetera or to investigate the environmental impact.

Acoustic plume noise has to be added to the list of mechanical loads that act on the space transportation system. For instance, Saturn V emitted acoustic power of about $2 \cdot 10^8\,\mathrm{W}$ [19], which corresponds to the power consumption of 200000 average homes. The angle of attack plays a major role in the dynamics of base region. The reattachment of the flow on the other hand, either on the nozzle wall (as shown in Fig. 1) or on the jet acting as fluidic wall has according to the investigations of Deprés et al. [20] no influence on the pressure distribution and spectral behavior in the base region. A jet temperature increase from $T_0 = 273\,\mathrm{K}$ to $800\,\mathrm{K}$ with a nozzle, which is immersed in the recirculation region, increases the base pressure by 15% as demonstrated by Zapryagaev et al. [21]. This in turn results in an overestimation of the base drag, which holds true to observations in real scale as shown with in-flight measurements conducted on *Ariane 5*. This insinuates that the simulation capability with appropriate jet temperatures is required.
With increasing altitudes and decreasing ambient pressure, the plume diameter increases. For a multiple nozzle space transportation configuration, the interaction of multiple plumes influences and distorts the flow pattern, and the altered heat transfer process may cause a low density region in the base, which may significantly influence on the drag. Systems for drag reduction and for the damping of buffet loads are under investigation.

An overview to heat sources is given in Goethert [22]. It is classified in (1) radiation caused by the exhaust gas and the rocket nozzle, (2) the recirculation of hot exhaust gases into the base region without *afterburning*, the (3) recirculation of fuel-rich exhaust gases with *afterburning* at the base and the interaction of exhausts or multiple nozzle effects. Simmons [23] describes the impact on the emissive properties if the hot exhaust gases carry soot particles like from hydrocarbon fuels, aluminum oxide from solid propellants or condensed particles. The particles flow exhibit a lag of velocity and temperature and causes a separation in the two-phase flow, which can alter the plume shape significantly [24]. The slow down of the typically fuel rich exhaust gases with incompletely oxidized fuel species in the shear layer of the ambient air and the jet causes a temperature recovery, which then promotes *afterburning* and IR emission. The recirculation region can here act as a flameholder and sustain this process. As described before, a multiple nozzle configuration lead at higher altitudes to the impingement and interaction of the separate jets, which causes hot gases to travel even upstream on the space vehicle [22]. The consequences are high temperature areas with the inherent effects of an increased emission, increased temperatures in the shock-heated air, the augmentation of hot backflow and upstream separation. The plume separated region can act under such circumstances as flameholder [25].
Further, Goethert [22] categorizes the significance of the different heat sources for a rocket in general. *Afterburning* dominates in the low altitude range up to an altitude of about $4.5\,\mathrm{km}$ ($15000\,\mathrm{ft}$). At medium altitudes at $4.5\,\mathrm{km}$ to $15\,\mathrm{km}$ ($50000\,\mathrm{ft}$), *afterburning* has a major contribution to heat loads and a significant part comes from the plume interference. The first diminishes completely for altitudes above $15\,\mathrm{km}$, while the latter is described as major. Additionally, recirculation of hot gases without *afterburning* for a multi-nozzle rocket configuration and radiation reaches a significant heat load level.

The plume trail is of great interest concerning environmental issues or the detectability and trackability of flight vehicle. The first relates to impact of the plume remains in the atmosphere and specifically in the stratosphere or ozone layer. The latter is described with the terminology rocket exhaust signatures and involves the subject of primary and secondary smoke, its classification, plume microwave and radiation properties. A better understanding understand of the mechanisms of smoke, soot, or vapor formation and the possibility to control them is required. One of the objectives is the minimization of radio-frequency interference and reduction of attenuation for specific antennas due to the plume. Kinefuchi et al. [26] reports of these effects for the Japanese M-V rocket and the European VEGA launch vehicle due to the usage of solid propulsion systems. In this regard, the rocket exhaust plume is seen as near field of the trail and starting point for further predictions of the trail [24].

Deposition and possible contamination of condensed species on the space transportation system and its components being optical surfaces, windows, solar panels or radiating heat emission surfaces due to plume impingement on vehicle is a further aspect of consideration. At high altitudes, the supersonic plume exhibits a Prandtl-Meyer expansion angles larger than $90°$ and the subsonic

boundary layer, although low, but not negligible in mass flow, can even travel further upstream with all associated issues induced by the exhaust gas.

The current revival of reusable launch vehicles and SpaceX efforts with the Falcon 9 Reusable Development Vehicle (F9R Dev) as shown in Ref. [27] opens up a less investigated field for future investigations. Firing in retro mode certainly involves many of the above described challenges, e.g. instabilities as shown in Ref. [28], over a wide Mach number range in a different fashion.

The aforementioned examples reveal that base region is an area of uncertainty in the current launch vehicle design process. In the past, base flow effects have mostly been examined in experiments with cold supersonic jets, which have shown to not mirror the base flow effects satisfactorily. The objective of the hot plume interaction facility is to provide a platform for the examination of base flow phenomena under realistic flight. Due to the importance of *Ariane 5* wrt the European space transportation system, the *Vulcain* engine, and thus oxygen and hydrogen, is chosen as baseline for the hot plume facility.

2.2. State of the Art and Future Developments

Various test benches with focus on investigating cryogenic injection and combustion phenomena are operated throughout the world with small scale combustion chambers. The objective of the work at hand is not on these phenomena, but the parameters of the test benches is used to get an idea about the classification of the future interaction facility. These test benches investigate combustion chambers, which correspond to applicable chamber with respect to the size. An exemplary overview about existing facilities is given in Tab. 1. It contains the *Cryogenic Combustion Laboratory* (CCL) of the *PennState University*, the *Mascotte* test bench of *Onera* and the small scale test facility *M3.1* of *DLR Lampoldshausen*.

To cope with potential future developments, the facility is designed to feature methane compatibility and operability. This is driven by recent efforts throughout the world towards methane/oxygen engines. Airbus Defence and Space Defense initiated LOX/Methane studies for rocket engines of a $350\,\mathrm{kN}$, $420\,\mathrm{kN}$ and $600\,\mathrm{kN}$ thrust class named ACE-35R, ACE-42R and ACE-60R, respectively, followed by sub-scale and equipment tests. It is stated that the engine demonstrator ACE-35R could be ready for test in 2018 Ref. [34]. Firing test of a European staged combustion engines are presented in Ref. [35]. In 2012, SpaceX announced the development of a methane-fueled rocket engine comparable in thrust with the F-1 engine of the Saturn V named Raptor. The Russian-based NPO Energomash company considers the modification of their RD-169, RD-182, RD-184, RD-185, RD-190 and RD-192 rocket engines to operate with liquefied natural instead of kerosene [36]. French/Russian activities are summarized in Ref. [37]. The future launcher preparatory program (FLPP) of ESA focuses the future demonstration work on two propellant combinations, one of which is LOX/methane [38, 39]. A general overview to the liquid propulsion systems and propellant choices is given in Ref. [40]. NASA, Aerojet and the German Aerospace Agency are mentioned to pursue activities in the respective field. Korea and Japan performed tests, which are described in Ref. [41, 42], respectively.

2.3. Scaling Considerations

The main parameters governing the base flow of a rocket were investigated by Goethert and Barnes [43]. Under the assumption of geometric similarity, it is concluded that non-viscous and viscous effects have to be considered.
Similarity for the non-viscous effects are satisfied: if (G-1) the static pressure change case by the a change in flow direction for full-scale vehicle and model is equal for the external flow, if (G-2) the static pressure change caused by a change in the flow direction for full-scale vehicle and model is met for the exhaust jet, and if (G-3) the ratio of the static pressure in the jet at the nozzle exit to the static pressure in the undisturbed external flow for the full-scale vehicle and the model is equal. The first two aspects relate to the pressure sensitivity of the external/jet flow with respect to the flow direction, which is required to be constant for both hot and cold flow. The non-viscous scaling rules (G-1 to G-3) were applied in Ref. [44] and have shown to find a good correlation for the base pressure between the hot and cold gas nozzle flows.
For the viscous effects, Ref. [43] considers the mixing process between the ambient flow and the exhaust jet as dominating and neglects the mixing process in the base region due to the small velocities, and thus only concerns the mixing of an essentially parallel flow. Two similarity parameters are developed: The *excess pumping mass* (G-4) parameter and the *total pressure at the jet boundary streamline* (G-5). The first is a measure for the entrained mass of the mixing layer, the second is required to provide similar discharge conditions.

More recently, Frey [45] suggested a scaling approach for *Ariane 5*'s point of maximum buffeting at Mach 0.7. It is based on shear layer similarity with respect to plume shape and entrainment arguing that the shear layer is the only way of interaction between the nozzle flow and the ambient flow. Consequently shear layer growth must be equal for flight and wind tunnel experiment. Six parameters describing the conditions directly at the nozzle exit are identified to govern this process: (F-1) The velocity of the plume, (F-2) the velocity of the surrounding external flow at the nozzle lip, (F-3) the density ratio between the external and plume flow, (F-4) the degree of turbulence of the internal flow, respectively the degree of turbulence of the boundary layer along the inside of the nozzle, (F-5) the angle between the shear layer direction and the nozzle axis, and (F-6) the nozzle lip thickness. The parameters refer to the location downstream from the nozzle lip, and respectively downstream from the pressure adaption of the nozzle resulting in a shock or expansion fan.
Further considerations a dedicated to the issue of reaching flight-comparably high jet exit velocities. Sensitivi-

Table 1. Operational parameters of exemplary test benches. The abbreviation (L) and (G) specify the state of the fuel/oxydizer as liquid and/or gaseous, respectively.

Test bench			CCL [29, 30]	M3.1 [31, 32]	*Mascotte* [33]
Total mass flow	$\dot{m}$	gs^{-1}	-	400 (L)	-
Mass flow oxygen	$\dot{m}_{O_2}$	gs^{-1}	450 (G/L)	-	$40-400$ (L)
Mass flow hydrogen	$\dot{m}_{H_2}$	gs^{-1}	113(G)	-	$5-75$ (G)
Pressure limit	$p_{CC,max}$	MPa	9.6	4	10

ties like the specific heat ratio, the influence of the molar mass of exhaust gas, gas temperature and mixing ratio are addressed with the goal to increase the exit velocity. It is concluded that the highest degree of similarity in terms of exit velocity is reached either by using helium, as being used in Ref. [46], or even better by operating a combustion chamber at a hydrogen rich mixture ratio of about 0.7. The latter yields at 82% of the *Vulcain* exit velocity in comparison to helium or cold air, which is at 56% and 15%, respectively. The low mixture ratio comes with the benefit for the materials used for the combustion chamber due to combustion chamber temperatures of about 1000 K.

2.4. Test Environment

In the current state, VMK as shown in (Fig. 2) is a blow-down type wind tunnel featuring a vertical free test section for tests in the subsonic to supersonic range starting from Mach 0.5 up to 3.2. The stagnation temperature can be adjusted up to 700 K and a stagnation pressure up to 3.5 MPa is possible. As a result, sea level conditions can be simulated up to a Mach number of 2.96. This and the operational range of VMK in terms of adjustable unit Reynolds number range for the various Mach numbers is shown in Fig. 3. Three different axis-symmetric nozzles with an exit diameter of 184 mm, 270 mm and 340 mm are available for subsonic tests. For supersonic tests, VMK facilitates tests with 14 axis-symmetric nozzles exhibiting an exit diameter of 150 mm, 230 mm and 310 mm.

Further, the test section of VMK is integrated in tower with a height of 11 m and a ground area of 4 m by 4m. The concrete walls have a thickness 70 cm and all structural elements like schlieren windows or steel doors are designed to be explosion-proof. Consequently, VMK is predestinated for wind tunnel experiments with propellants and explosives, which is shown in the long history of experiments regarding side jets with solid propellants (e.g. Ref. [47, 48]) or ram jets (Fig. 4) with integrated and realistic combustion chambers fueled with various propellants like hydrogen, carbon based propellants or others. Recently, the range of applications for VMK was extended to investigate hovering re-entry capsules in free flight as examined for the MarcoPolo-R ERC capsule [49, 50]. The paper at hand summarizes the ongoing work progress to extend VMK's capabilities to

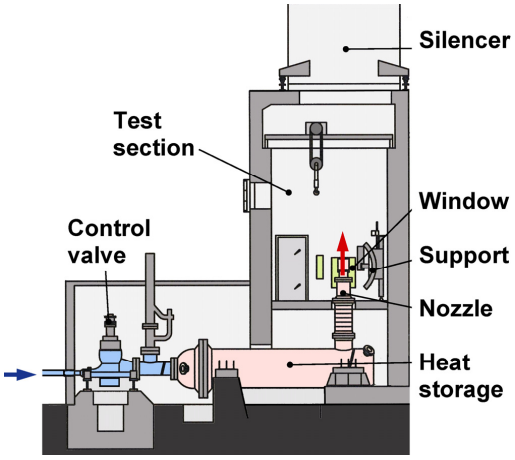

Figure 2. VMK facility components.

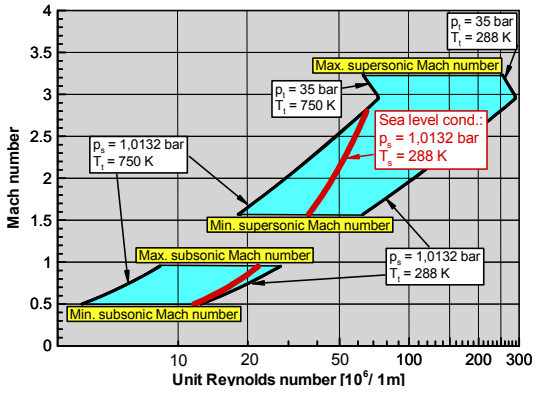

Figure 3. Reynolds number range of VMK facility.

Figure 4. Exemplary propulsion test of a RAM-jet configuration in VMK.

perform hot plume tests with gaseous hydrogen/gaseous oxygen combustion for the simulation of thermal and mechanical loads on the base of space transportation vehicles during the ascent with focus on the most critical part, which is transonic flow regime. As reference for planned hot plume interaction facility in Cologne serves the main stage of *Ariane 5* with its *Vulcain* engine since it is the main European space transportation system. In the past, experiments were performed with the solid propellant combination based on HTPB/AP/Al as used in the EAP boosters of *Ariane 5*. In the future, this upgrade empowers experiments in VMK to study generic single plume effects with various propellants and complete *Ariane 6*-like configurations with plume-plume interaction and the resulting effects on the structure. Additionally, the methane compatibility of the facility covers possible future developments as discussed in industry and various international space agencies. Consequently, base flow experiments can be run for all current and possible future members of the European space launcher family. This includes *Vega*, *Ariane 5*, *Ariane 6* and most *FLPP* studies.

The upgrade of the hot plume testing facility can be divided in several steps. Step 1: The realization of the hydrogen/oxygen supply system is scheduled for 2015/2016. Subsequently, experiments can directly be conducted after the manufacturing of a combustion chamber and integration in a already partially existing wind tunnel model from investigations conducted by Emunds and H. Riedel [51]. The targeted diameter for the representation of the main stage is in correlation with these previous experiments at $67\,\mathrm{mm}$ for a subsonic wind tunnel nozzle with $340\,\mathrm{mm}$.
As a mid-term plan (step 2), it is planned to equip VMK with a larger subsonic wind tunnel nozzle of the size of $600\,\mathrm{mm}$. This makes the $1:1$ integration of the *PennState* combustion chamber with an external diameter of $148\,\mathrm{mm}$ in the wind tunnel model seem reasonable. The *PennState* burner was selected for several reasons. Among others since it is run with gaseous oxygen and gaseous hydrogen up to the stoichiometric mixture ratio, since it is considered to be a benchmark test case, and thus well experimentally [29] and numerically [52] investigated and documented. For instance, details to the dimensions of the combustion chamber and injector are given in Ref. [30]. The CFD in Ch. 4 is based on this upgrade step 2.
The realization of step 3 falls also in the range of mid-term planning. The department is currently studying opportunities to reduce the ambient pressure in the measurement section. This aspect is advantageous with respect to the adjustment of the pressure ratio between the external and nozzle flow and basically allow altitude simulation like during the ascent of space transportation systems.
In the long term (step 4), the principle of the upstream support concept will also be applied for supersonic testing. This can be done with appropriately designed wind tunnel nozzles as shown for example in Ref. [53, 54]. Independently from step 4, classical strut supported configuration can easily be test with the existing supersonic wind tunnel nozzles of VMK.

The developments and experiences for VMK will be used as blueprint to establish hot plume testing capabilities in *Trisonic Test Section Cologne* (TMK) [55, 56] in Cologne. This facility is equipped with a transonic test section with perforated walls for an improved flow quality. Perturbations coming from free jet shear layer of an open test section as described by Weiss and Deck [57] can be avoided this way. Further advantages lay in the possibility to adjust the static pressure in the measurement section with little modification for altitude simulations, the possibility to change the angle of attack/yaw and experiments can be conducted continuously from Mach 0.5 to 5.7. The comparison of experiments in both facilities provide insights into the influence of the support.

3. METHODS

A justification for a hot plume facility was given in Ch. 2. The subsequent question to clarify is how to establish similarity to flight. An introduction to the scaling issue was given in Ch. 2.3 based on the work by Ref. Goethert and Barnes [43] and Frey [45]. The two scaling approaches are opposed to each other and evaluated in Ch. 3.1 to find appropriate parameters that reflect similarity to *Ariane 5* over the complete transonic Mach number range. For this task, it is necessary to make realistic assumptions, which is based on existing

hardware. The *PennState* burner was chosen as reference for the hot gas generation. It is run at maximum chamber pressure of $6.89\,\mathrm{MPa}$. For comparison: *Vulcain 2* operates at $\sim 12\,\mathrm{MPa}$. The wind tunnel VMK in Cologne is taken as a given second prescription. Note that the static pressure at the exit is always the ambient pressure due to the open test section environment. In Ch. refchap:TestEnvironment, it is made use of the scaling assessment to define the reference conditions for the future facility. The DLR TAU code and the applied method is described in Ch. 3.3.

3.1. Scaling Considerations

The non-viscous scaling parameter of Goethert and Barnes [43] referring to the static pressure change of the nozzle supersonic model flow (G-2) can be expressed as a function of Mach number and heat capacity ratio. For hot gas tests with comparable mixture ratios to flight, it essentially reflects Mach number similarity for the nozzle flow if the latter is matched. But, this similarity parameter is difficult to keep since, on the one hand, the combustion chamber pressure must be large enough to avoid the violation of the pressure ratio (G-3) and to avoid a significant alteration of the plume pattern or even flow separation in the model nozzle. On the other hand, the maximum chamber pressure is limited in order to handle the heat flux especially at throat of the nozzle for small burners. Consequently, the exit Mach number, ergo the expansion ratio, is adapted to match the pressure ratio condition G-3. The pressure change condition G-1 for the ambient flow is imposed by keeping the Mach number $M_{\infty,Exp} = M_{\infty,Ariane}$ similar. This can easily be set for wind tunnels by adjusting the stagnation pressure (for a subsonic nozzle).
The viscous scaling parameters require the displacement streamline, which is modeled as function of the jet's Mach number M_∞. Further input parameters for the *excess pumping mass* (G-4) and the *total pressure head* (G-5) are only the density and velocity of both the jet and the ambient flow.

The similarity parameter of Ref. [45] include parameters, which are dependent on the specific behavior or geometry of the wind tunnel model. Thus, the degree of turbulence (F-4) and the nozzle lip thickness (F-6) are not taken into account for the design at the current state. The other parameters find their equivalence. The velocity condition F-1 and F-2 are comparable to the Mach number similarity M-1 and M-2, respectively, and the angle of the shear layer direction (F-5) is driven by the pressure ratio (G-3). For the design of the facility, the intention is not to find a wind tunnel model with high degree of similarity to the wake flow of *Ariane 5* with a similar exhaust plume. The idea is rather to show the potential of the hot plume system in combination with VMK over a wide Mach range of the transonic flow regime.

The methodology to judge similarity is to determine the nozzle exit and ambient properties (p, ρ, v,ρv, T) during the ascent of *Ariane 5* and set them in relation to the properties of the nozzle exit and ambient properties of the planned experiments. The ratio of both is equal to 1 for all properties if the conditions are identical.
In more detail, the idealized nozzle exit parameters for *Ariane 5* and *PennState* burner plus defined nozzle were calculated with *Rocket Propulsion Analysis* [58]. The *Ariane 5E H173* version as given in Ref. [59] was taken as reference. The trajectory and the corresponding parameters during the ascent was calculated with the trajectory simulation program (Ref. [60]) for *Ariane 5*. It returns, among other parameters, the velocity as function of altitude. By means of the atmospheric data, in the case here the U.S. standard atmopshere [61], the static gas properties and the velocity were converted and linked to the Mach number, which are of concern for the experiments. The static gas properties of the wind tunnel are defined for all Mach number due the pressure adaptation at the nozzle exit for the subsonic case of concern. As it can be seen in Fig. 3, the temperature is variable. For subsonic tests, this is unusual, thus the reservoir pressure is set to $288\,\mathrm{K}$.

3.2. Test Environment

In order to receive an estimated maximum and minimum mass flux for the hot plume testing facility, a combustion chamber had to be found or designed, which can be integrated in a wind tunnel model. A literature research revealed that the *PennState* burner is suitable combustion chamber to continue the study. It corresponds to the dimensional limitations, is well documented, features *Vulcain 2*-like combustion chamber condition and a co-axial injector, which is of relevance for rocket engine application. More to the reasoning is given in Ref. [62].

The outer diameter of the VMK wind tunnel model is approximated as follows: The throat diameter of the *PennState* burner, the expansion rate of the *Vulcain 2* engine and the *Ariane 5*-like diameter ratio between the diameter of the main body and the diameter of the nozzle of 0.4 is used to calculate the inner nozzle exit diameter and the diameter of the main body. It accounts to $61.2\,\mathrm{mm}$ and $158\,\mathrm{mm}$ (including a nozzle thickness of $2\,\mathrm{mm}$), respectively. The outer diameter of the *PennState* burner is in a comparable range ($148\,\mathrm{mm}$). Note that this is an imaginary model and this approach is used to determine the maximal outer diameter. Such a configuration would require a very high combustion chamber pressure to avoid nozzle flow separation. This in turn causes very high heat loads on the model.

Three reference conditions (RC 0 to RC 2) are defined to cover the operating capabilities of the facility. Reference conditions RC 0 defines a 'cold' and low pressure condition, RC 1 is a 'must' condition to cover the capabilities of the *PennState* burner, and RC 2 is based on a maximum, 'nice-to-have' scenario. No attention is paid to the question if the heat loads of RC 2 condition can actually be managed for this exact configuration. The idea

is to enable experiments like this with the hot plume interaction facility and to cover a broader range of potential experiments with to date undefined configurations.

In detail, RC 0 is a hydrogen-rich condition with a mixture ratio of 0.7 at a chamber pressure of $2.07\,\mathrm{MPa}$ for a nozzle throat diameter of $8\,\mathrm{mm}$. Experiments with condition RC 0 reach very high exit velocities, meaning high similarity in that respect, at moderate demands on the materials. According to Ref. [45], the exit velocity can go up to $u_{max} = 3467.1\,\mathrm{ms}^{-1}$ for expansion in vacuum, which corresponds to 82.0% of the *Ariane 5*'s exit velocity. Special precautions for heat management can be circumvented and thus, a wind tunnel model featuring such a combustion conditions can easily be integrated in TMK. Condition RC 1 is specified by a chamber pressure of $6.89\,\mathrm{MPa}$, a mixture ratio of 6.0 and a nozzle throat diameter of 8.0. An expansion ratio of 20 is an additional requirement to avoid nozzle flow separation during the experiments (for flow separation see e.g. Ref. [14]). Condition RC 2 is motivated by two different drivers. The first driver is the desire to conduct experiments in a pressure range, which is comparable to Ariane 5, meaning up to $\sim 12\,\mathrm{MPa}$. The second driver corresponds to the requirement to test RC 1 condition for a nozzle diameter that allows similarity with respect to the outer geometric scaling between Ariane 5 and the wind tunnel model. The outer diameter of the VMK model ($158\,\mathrm{mm}$) leads with geometric outer scaling and an expansion ratio of ~ 20 to a nozzle throat diameter of about $13.7\,\mathrm{mm}$. The resulting mass flows of these reference conditions are listed in Tab. 2. Obviously, if the mass flux is held constant, RC 2 defines the upper limit of the operating range.

The aforementioned reference conditions are valid for the *operational mode*. Additionally, ignition conditions IC must be specified for the *ignition mode*. The idea is to ignite the combustion chamber through a nozzle with a flare system. The *ignition mode* targets at low pressures and low a mixture ratio to avoid a pressure overshoot and to keep the heat loads low in that phase. To be on the secure side with the ignition through the nozzle, it is intended to stay below conditions that lead to a choked nozzle flow. In discussion with industry, the minimum mass flow for the supply system (see Ch. 4) was determined and documented (Tab. 2). This minimum mass flow is considered as sufficient. Ignition with a mixture ratio of 2 and a combustion chamber pressure of $0.16\mathrm{MPa}$ can be realized with nozzles exhibiting a throat diameter from $4.2\,\mathrm{mm}$ to almost $24.5\,\mathrm{mm}$.

This statement is supported by literature on ignition. Hasegawa et al. [63] successfully conducted laser ignition experiments for comparable parameters and conditions, meaning a mixture ratio $O/F = 2$, combustion chamber pressures ranging from $0.15\,\mathrm{MPa}$ to $0.35\,\mathrm{MPa}$ and a throat diameter of $d_{th} = 3\,\mathrm{mm}$. The calculated hydrogen mass flow ranges from $0.14\,\mathrm{gs}^{-1}$ to $0.33\,\mathrm{gs}^{-1}$. An anchored flame was observed by Schmidt et al. [64] for a nozzle with a throat diameter of $4\,\mathrm{mm}$, a mixture ratio of about 2 and a hydrogen mass flow of $0.58\,\mathrm{gs}^{-1}$.

3.3. Computational Fluid Dynamics

Computations are carried out using the DLR TAU Code. It is discussed in detail in the literature see e.g. Ref. [65, 66]. TAU is a hybrid grid, finite volume second order accuracy flow solver. It has been validated for a variety of steady and unsteady flow cases, ranging from sub to hypersonic Mach numbers Ref. [67, 68].
As the investigated geometries are essentially axis-symmetric in this work, all computations are carried out in two dimensions under assumption of axisymmetry. For this initial study, the involved gases are treated as a mixture of non-reacting ideal gases. Species accounted for are H2, H, O2, O, H2O, OH, HO2, H2O2, and N2. The reservoir composition inside the combustion chamber is computed with NASA's "Chemical Equilibrium and Applications" (CEA) code by Gordon and McBride [67, 68]. The combustion chamber is simulated to operate with a pressure of $11.9\mathrm{MPa}$ at $3669\,\mathrm{K}$ and species corresponding to a mixture ratio of 7.1. The flow is released through a Vulcain 2 nozzle (scaled to fit on the wind tunnel model concept) in the ambient Mach 0.86. The stagnation pressure and temperature of the facility is set to $0.164\,\mathrm{MPa}$ and $288\,\mathrm{K}$, respectively. Since an open test section is simulated, the ambient pressure is initiated with $0.102\,\mathrm{MPa}$.

3.4. Measurement Techniques

The requirements for a suitable selection of measurement techniques for the proposed concept are listed in the following. In detail, the test section diameter and length is according to the planned dimensions of VMK at $600\,\mathrm{mm}$ and a run time of the facility between $2\,\mathrm{s}$ and $50\,\mathrm{s}$ is assumed. In the transonic range, the free stream velocity and Mach number is in the range of $160\,\mathrm{ms}^{-1}$ to $360\,\mathrm{ms}^{-}1$ and 0.5 to 1.2, respectively, at a free stream pressure of about $1\,\mathrm{bar}$. The diameter of wind tunnel model is in the range of $50\,\mathrm{mm}$ to $160\,\mathrm{mm}$, while the wind tunnel nozzle diameter is about 40% of the model diameter. The exhaust jet velocity and Mach number was specified to be between $3000\,\mathrm{ms}^{-1}$ and $4400\,\mathrm{ms}^{-1}$ at an exhaust jet static temperature of $340\,\mathrm{K}$ to $2000\,\mathrm{K}$.

4. RESULTS AND DISCUSSION

4.1. Scaling considerations

Reynolds number similarity is demanded for most simulations in aerodynamics. Fig. 5 depicts the unit Reynolds number Re_U of a representative ascend trajectory of *Ariane 5 ECA* as function of the ambient Mach number Ma_∞ (Ref. [60]). The altitude H is given additionally to explain the influence of the atmosphere. It can be seen that the Reynolds number increases steadily due to the increasing velocity of the vehicle. The maximum is reached at $Ma_\infty = 0.82$ at an altitude of $4.5\,\mathrm{km}$, which

Table 2. Reference conditions for operational (RC0-RC2) and ignition mode (IC).

Reference condition			RC 0	RC 1	RC 2	IC
Combustion chamber pressure	p_{CC}	MPa	2.07	6.89	11.5(15)	-
Mixture ratio	O/F		0.7	6.0	6.0	-
Total mass flow	$\dot{m}$	gs^{-1}	89.2	150.3	440.8	-
Mass flow oxygen	$\dot{m}_{O_2}$	gs^{-1}	52.5	128.8	377.8	0.6-20
Mass flow hydrogen	$\dot{m}_{H_2}$	gs^{-1}	36.7	21.5	63.0	0.3-10

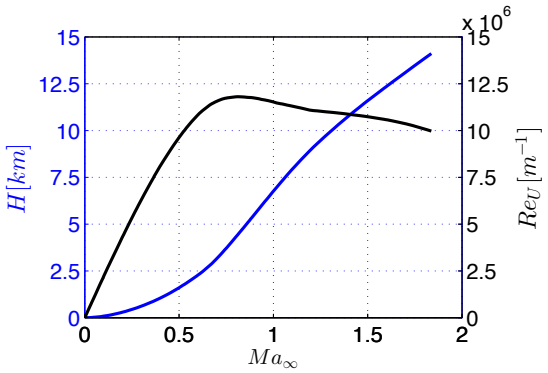

Figure 5. Exemplary Ariane 5 *ascend. Altitude and unit Reynolds number over Mach number.*

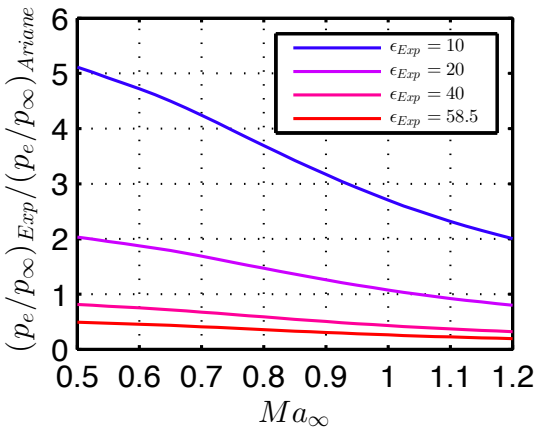

Figure 6. Pressure ratios between experiment and flight over Mach number for various expansion ratios.

is mainly invoked by a temperature curvature change in the atmosphere. Taking into account the differences of the base diameter as characteristic length scale between flight and experiment of about two orders in comparison with the operational range VMK (Fig. 3), it becomes clear that the Reynolds number is impossible to match for such a configuration with experiments in VMK. For more details, see Ref. [16]. In the previous similarity studies in Ref. [43, 45], the Reynolds number did not occur as influential parameters. To answer the question about its influence, literature on wake flows is consulted. The base pressure is taken here as reference. On the one hand, since it was on the focus of many investigations for a long time, and on the other hand, since it seems to be a governing parameter as shown before. Note that this is a necessary, but not a sufficient criteria for flow similarity.

Murthy and Osborn [69] assembled a bibliography about base flow phenomena and presents various correlations approaches. The Reynolds number is explicitly mentioned in the *Kurzweg Correlation* and *Love Correlation*. It is stated that for wake flows without injections/jets, the Reynolds number has an negligible influence on the base pressure as long as the incoming boundary cylinder on the main body is turbulent. In Ref. [69], an influence is attributed to the Mach number, angle of attack, boundary layer thickness and boundary layer characteristics and surface temperature. Experiments conducted by Zapryagaev et al. [21] in the recent past show the same insensitivity to Reynolds number variations. The other influences should be kept in mind for the final definition of the wind tunnel model for a potential adjustment of the boundary layer with appropriate measures like boundary suction, blowing, roughness elements or surface temperature adjustments.

For the further discussion, the Reynolds number is consequently neglected. 'Screws' that can be changed to adjust the similarity for a predefined Mach numbers are the stagnation temperature of the wind tunnel, and for the combustion chamber the pressure, the expansion ratio of the nozzle and the expansion ratio. The sensitivity of these parameters has been evaluated in Ref. [16] and an excerpt is shown in Fig. 6 to Fig. 10. Based on the discussed approach, it shows the individual gas property ratio of the nozzle exit and the ambient flow of the experiments in relation to *Ariane 5*-like conditions as function of the simulation Mach number for different expansion ratios. As baseline, the combustion chamber of the wind tunnel model is set to $6.89\,\mathrm{MPa}$ (*PennState*), a mixture ratio of 6 and an expansion ratio of 58.5 (red line).

It shows that by varying the expansion ratio, the pressure ratio (see Fig. 6) - the essential parameter for plume formation (G-1/F-5) - can be kept similar over a wide range without having a significant influence on the velocity ratio (Fig. 7). The ratios with respect to density ratio

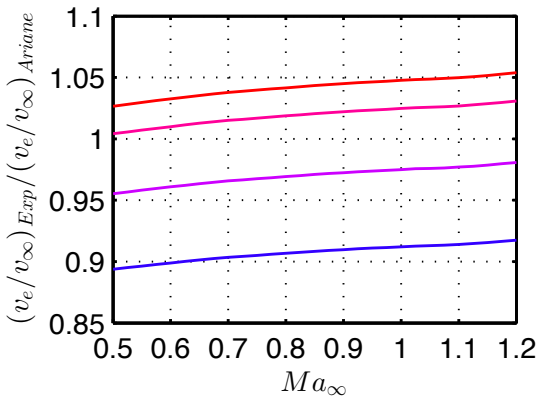

Figure 7. Velocity ratios between experiment and flight over Mach number for various expansion ratios.

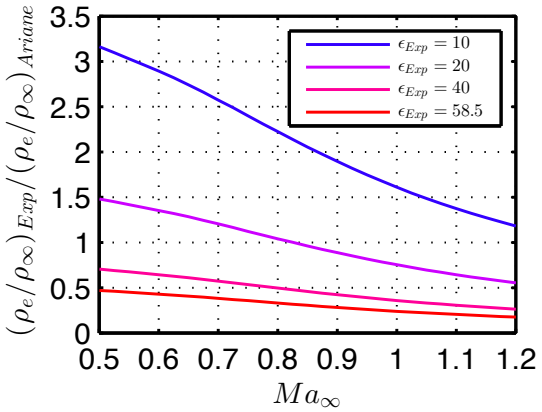

Figure 8. Density ratios between experiment and flight over Mach number for various expansion ratios.

(Fig. 8), impulse density ratio (Fig. 9) and temperature ratio (Fig. 10) can be kept in the same order. It seems like an expansion ratio of $\sim$ 20 can lead to comparable results. As mentioned before, these parameters are used to determine the operational conditions for the future facility. If similarity is required at a specific Mach number, a detailed analysis with respect to the viscous behavior of the plume is required.

The influence of the other 'screws' is studied in Ref. [16]. It shows that a change of mixture ratio between $O/F = 4$ to 8 does not offer this wider range of comparable ratios. Mainly the temperature ratio can be influence while the other ratios stay in a very narrow regime. An adjustment of the pressure ratio is not possible this way and flow separation in the nozzle has to be expected (Ref. [14]). This can be avoided by increasing the combustion chamber pressure to a most likely detrimental level of 15 MPa, which is also advantageous for the density and impulse density ratio while keeping the temperature and velocity ratio at a comparable level. Note that mixture ratio 'screws' is also changed without considering the effect on an existing set-up. The parameter variation shows that the most favorable parameter to adjust is the expansion ratio since it can be changed without increasing the loads on the combustion chamber.

4.2. Test Environment

The proposed concept shown in Fig. 11 is a combination of the wind tunnel model used by Emunds and H. Riedel [51] for base flow investigations and the *PennState* burner [29] or slightly modified, but similar burner [62]. Bos et al. [70] presented a comparable concept with respect to the support in their feasibility study for a hot plume test facility. Upstream of the nozzle exit, the wind tunnel nozzle (1) is equipped with support arms (2), which have three tasks: They simply keep the wind tunnel model in place, the upper and lower support arm supply the com-

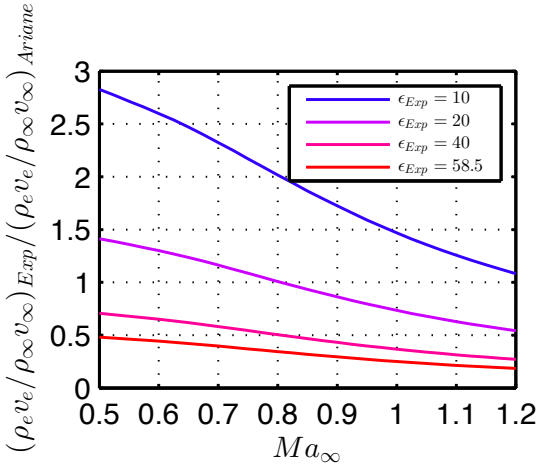

Figure 9. Impulse density ratios between experiment and flight over Mach number for various expansion ratios.

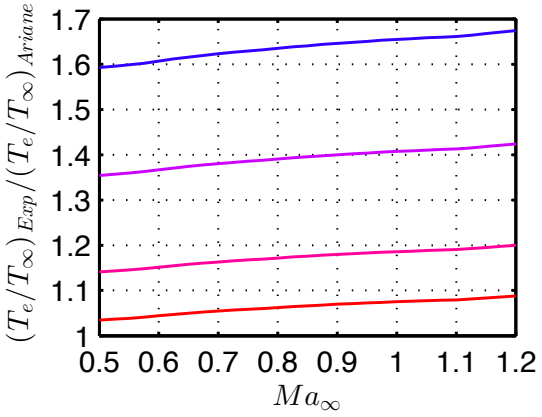

Figure 10. Temperature ratios between experiment and flight over Mach number for various expansion ratios.

bustion chamber with gaseous hydrogen (3) and gaseous oxygen (4), respectively, and a one or several hydrogen supports can be selected as exit of the sensor harness. The support arms converge in a central mounting (5) on top of which is the combustion chamber (6). The injector (7) and the nozzle (8) is exchangeable to realize various injection conditions and nozzle exit conditions, respectively. The wind tunnel nozzle is equipped with two levels of straighteners (9) downstream of the support arms to minimize perturbations. Fig. 2 shows the location of the assembly with respect to the wind tunnel. This upstream supported concept is advantageous since streamlines of the upstream part of the wind tunnel model can not be 'squeezed', and the flow can not be accelerated to Mach 1. Thus, blockage [71] is no issue and the diameter can be freely selected. Further, the upstream support minimizes disturbance, which usually induced from a strut support. On the other hand, Weiss and Deck [57] showed that the shear layer of the wind tunnel model influences the pressure fluctuations and has to be taken into account by CFD and/or the diameter has to be sufficiently large with respect to the model in order to allow the negligence of these disturbance.

For upgrade step 1, the ratio between the wind tunnel model and the model is $\phi/D = 340\,\mathrm{mm}/67\,\mathrm{mm} \approx 5.1$. For upgrade step 2 with the increased wind tunnel nozzle ($\phi = 600\,\mathrm{mm}$), it is at $\phi/D \approx 9.0$. It is expected that the influence of the shear layer perturbation decreases if this ratio is about twice or four times as large as for the investigations conducted by Ref. [57]. These calculations were conducted with $\phi/D \approx 2.86$.

The supply of the wind tunnel model is executed as shown in Fig. 12. It shows the process flow diagram of the GOX/GH2 supply from the storage outside of the building to the combustion chamber in the test section in accordance with the previously defined reference conditions. It basically consists of a GOX line, a parallel GH2 line and a nitrogen line for purging different segments of the supply system. The facility essentially runs in two different modes: *Ignition mode* and *operational mode*. In the *ignition mode*, the mass flow is passing through the pressure reducing valves DR-X04/DR-H04, which limits in combination with the setting for the control valves CV-X07/CV-H07 the mass flow for a secure and 'low' pressure ignition. A flare system is used for ignition and for burning excess-gas. Optionally, other system can be integrated in the system as well. In the *operational mode*, the mass flow passes through the shut-off valves AV-X06/AV-H06. The mass flow sensor at FT-X15/FT-H15 sends the mass flow rate to the *flow indicator and controller* FIC, which adjusts the control valves CV-X07/CV-H07 to the setpoint mass flow for the combustion chamber. Shutdown off the combustion chamber is realized by purging the combustion chamber. In case of emergency, the test section of the wind tunnel and the supply system is vented with nitrogen. The extra loop in the oxygen piping system prevents excessive and detrimental flow velocities during start-up.

The reference conditions in Tab. 2 were used as basis to

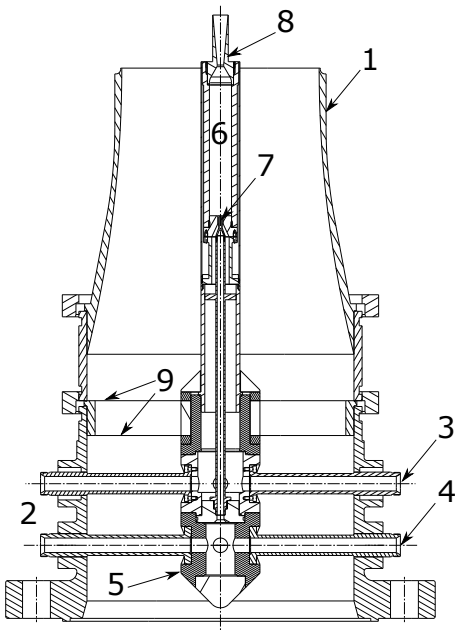

Figure 11. Cross-sectional view of the wind tunnel model concept.

specify the piping of the feeding system, which will obviously be assembled with standardized components. The next standardized step to include RC 2 condition is at $160\,\mathrm{MPa}$. This is the upper pressure limit for the feeding system. The selected pipes are rated for maximum volumetric flow rate of $0.0358\,\mathrm{m^3 s^{-1}}$ and $0.0029\,\mathrm{m^3 s^{-1}}$ for hydrogen and oxygen, respectively. Consequently, the maximum permitted mass flow is $\sim 480\,\mathrm{g s^{-1}}$ for hydrogen and $\sim 620\,\mathrm{g s^{-1}}$ for oxygen. In the invitation to tender, it is specified that the facility is required to adjust the mass flow to the nominal value with an accuracy of $\pm 5\%$ within $3\,\mathrm{s}$ from *ignition mode* and reaches an accuracy of $\pm 1\%$ within $6\,\mathrm{s}$. The hot plume testing facility offers a large enough margin to RC 2 and a high degree of flexibility is given to realize advanced experiments. Additionally, the facility compares well to the facilities presented in Tab. 1 and can be classified as intermediate-range test bench.

In a typical test sequence, the combustion chamber is ignited with a flare system (*Igntion mode*). After a stable combustion is detected, the facility is switched to the *operational mode* where the chamber pressure is increased to an intermediate set point to establish choked flow conditions in the model nozzle. The goal is to minimize coupling effects induced by the start of the wind tunnel, which is the next step. When the test conditions are set, the chamber pressure is increased to the nominal value. After the experiment, both systems are shut down simultaneously.

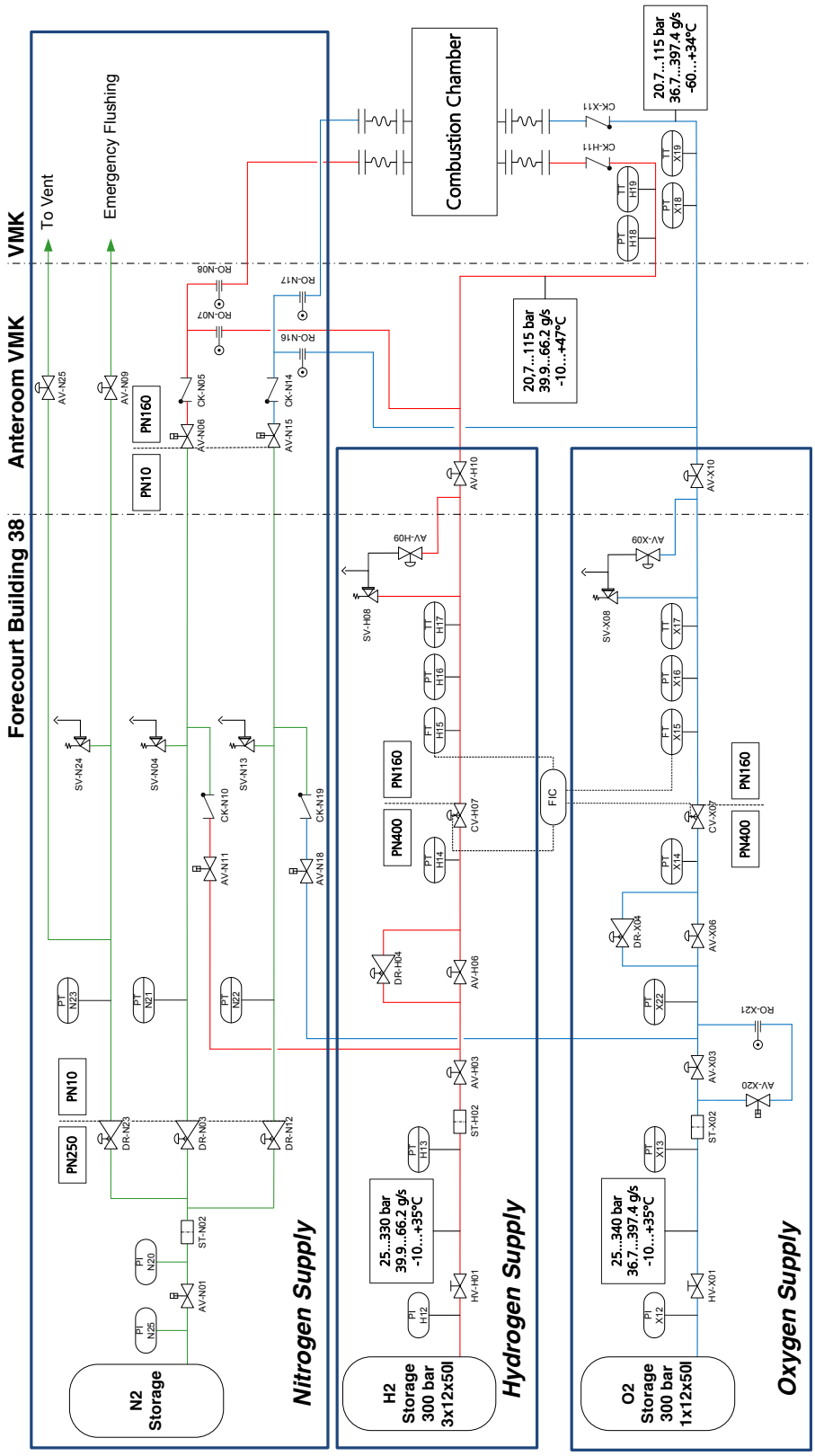

Figure 12. Process flow diagram for the GOX/GH2 supply.

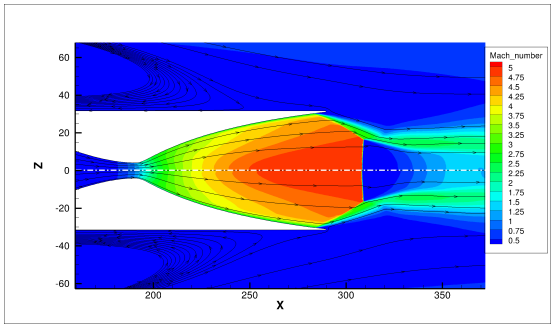

Figure 13. Comparison of Mach number contours of facility (top) and free flight (bottom) case, detail of rocket plume.

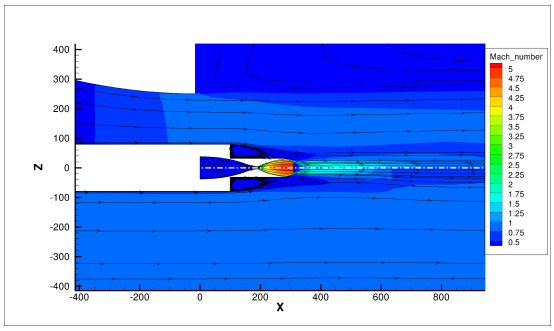

Figure 14. Comparison of Mach number contours of facility (top) and free flight (bottom) case.

4.3. Computational Fluid Dynamics

The wind tunnel concept presented in the previous section is opposed to free flight conditions here. The Mach number contours of the resulting flow fields are compared in Fig. 13 and Fig. 14. Fig. 13 demonstrates how the fundamentally different flow fields nonetheless lead to practically indistinguishable flow conditions at the rocket base. It can be seen in Fig. 14 that the base recirculation, the nozzle separation, and the position of the Mach disc are practically identical in both cases.

In order to allow a qualitative comparison, profiles are extracted in radial direction at three positions: at the wind tunnel nozzle exit and at both $0.5 \cdot R$ and R behind the rocket nozzle, where R is the rocket nozzle radius. It can be seen in Fig. 15 that the wind tunnel nozzle has been well designed. The boundary layer profile stopping to early is a data extraction artifact, the velocity reduces to zero at a no-slip boundary. The boundary layer profiles differ slightly. This might be due to the free flight case having a homogeneous build-up in a constant pressure environment, whereas the flow is accelerated through the wind tunnel nozzle. The difference in velocity at the nozzle exit is negligible, the shear layer develops slightly differently, possibly due to the difference in boundary layer profile. Overall agreement between both cases is in terms

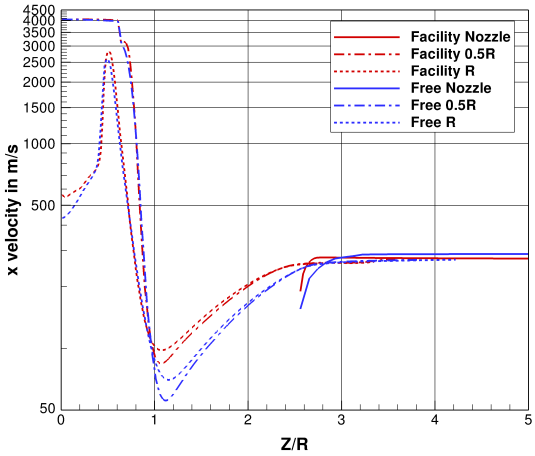

Figure 15. Radial profiles of axial velocity of free flight (Free) and facility (Facility) case.

of density is satisfactory as well. This can be seen in Fig. 16.

4.4. Measurement Techniques

For a coherent examination of the study, applicable measurement techniques are discussed in a last step. Willert et al. [72] studied relevant optical measurement techniques, ergo non-intrusive image based methods. Under consideration were flow field diagnostics like *Particle Image Velocimetry* (PIV), *Doppler Global Velocimetry* (DGV) and optical diagnostic methods for reacting flows like chemiluminescence, *Laser Induced Flouresscence* (LIF), *Filtered Rayleigh Scattering* (FRS) and *Coherent Anti-Stokes Ramann Scattering* (CARS). As a result, a combined single line OH-LIF and PIV measurement technique according to the work of Lange et al. [73] was recommended, which offers correlated information about temperature and velocity field with a high, two-dimensional spatial resolution on a single shot basis. Additionally, FRS [74] is considered to be advantageous as border crossing application for the temperature measurement in the recirculation region where the OH concentration is unknown and temperatures in the range of the ambient free stream are expected. OH-LIF is restricted to an OH concentration in the order of 0.1 to $2 \times 10^{16}\,\mathrm{molecules\,cm^{-3}}$ [73]. Constraints might arise for measurements close to the region with the bright hydrogen-oxygen combustion and due to the limited knowledge about this technique in the high temperature range [75]. The diagnostics can easily be complimented with measurement techniques, which are read to go at the department like high-speed Schlieren imaging, IR-thermography, spectroscopy in the IR, UV and visible range, steady and unsteady pressure measurements et cetera.

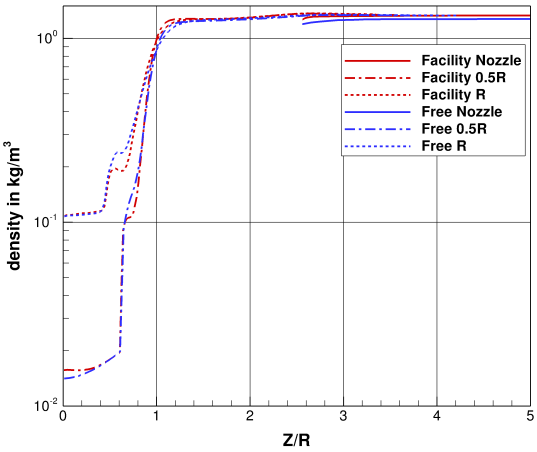

Figure 16. Radial profiles of density of free flight (Free) and facility (Facility) case.

5. CONCLUSION

The study at hand presents how to extend the capabilities of the existing wind tunnel *Vertical Test Section Cologne* to simulate representative experiments for space transportation systems in the transonic regime. An overview was given to the issues and challenges like buffeting, drag and heat loads for instance, and a conceptual solution was suggested by integrating the *PennState* combustion chamber in an upstream-supported wind tunnel model. The wind tunnel model is supported upstream to minimize strut disturbances and to transonic effects due to blockage. For this exact configuration, it was shown the highest degree of similarity over a wide Mach number range is most likely established by an adjustment of the expansion ratio to about 20. A more profound study based on the similarity rules of Ref.[43] for the viscous behavior or with an axis-symmetric shear layer model that takes compressibility, different gas compositions and temperature effects into account is necessary if investigations for specific flow conditions are required. Proof of concept was given by means of CFD simulations. The influence of the wind tunnel nozzle on the mean base flow is negligible. Further investigations are recommended to evaluate the influence of the wind tunnel nozzle shear layer on the unsteady base flow phenomena for a larger aspect ratio as investigated by Ref. [57]. The requirements of the feeding system were defined, which are set to a maximum mass flow rate of $\sim 480\,\mathrm{gs}^{-1}$ for hydrogen and $\sim 620\,\mathrm{gs}^{-1}$ for oxygen at a maximum pressure of $16\,\mathrm{MPa}$. By means of a process flow diagram, the realization of such a facility was discussed. The study concludes with an introductory description of a typical test sequence.

ACKNOWLEDGMENTS

This project is financially supported by the German Research Foundation (Deutsche Forschungsgemeinschaft – DFG) within the Transregional Collaborative Research Centre 40 (Sonderforschungsbereich Transregio 40). The help and advice of the technical staff of the *Supersonic and Hypersonic Technology Department* in Cologne is gratefully acknowledged.

REFERENCES

[1] Arianespace. Press conference to Flight 157 - Ariane 5 ECA, Paris, January 7, 2003.

[2] ESA. Arianespace Flight 157 - Inquiry Board Submits Findings. URL `http://www.esa.int/Our_Activities/Launchers/Arianespace_Flight_157_-_Inquiry_Board_submits_findings2`.

[3] K. Triesch and E.-O. Krohn. *Die Vertikale Meßstrecke der DFVLR in Köln-Porz (Stand 1986), DFVLR-Mitt. 86-22*. Wissenschaftliches Berichtswesen der DFVLR, ISSN 0176-7739, Postfach 906058, 5000 Köln 90, 1986.

[4] Vertical Test Section Cologne (VMK), Supersonic and Hypersonic Technology Department. URL `http://www.dlr.de/as/en/desktopdefault.aspx/tabid-194/407_read-5445/`.

[5] P. Leroux. Ariane 5 - Data relating to Flight 202. Launch kit, May 2011.

[6] *Ariane 5 User's Manual*. Number No. 3. Arianespace, 2000. URL `http://books.google.de/books?id=CbA0mwEACAAJ`.

[7] S. David and S. Radulovic. Prediction of Buffet Loads on the Ariane 5 Afterbody. In *In 6th Symposium on Launcher Technologies, Munich, Germany, 8-11 November 2005*, 2005.

[8] H. Wong, J. Meijer, and R. Schwane. Experimental and Theoretical Investigation of Base-Flow Buffeting on Ariane5 Launch Vehicles. *Journal of propulsion and power*, 23(1):116–122, 2007.

[9] J.J. Meijer and C.M. van Beek. Analysis of Ariane 5 Base Flow Measurements in the NLR-PHST and FFA T1500 Wind Tunnels. *National Aerospace Laboratory, NLR-CR-99449*, 1999.

[10] H. Wong and R. Schwane. Final Report on Numerical Support to Aerodynamics Buffeting Problems in Ariane5. *European Space Technology and Research Centre, Doc. YPA/2236/HW*, 1997.

[11] J. Muylaert, W. Kordulla, D. Giordano, L. Marraffa, and R. Schwane. Aerothermodynamic Analysis of Space-Vehicle Phenomena. *ESA bulletin 105, Aerothermodynamic Analysis*, 2001.

[12] H.V. Fuchs, E. Mercker, and U. Michel. Large-Scale Coherent Structures in the Wake of Axisymmetric Bodies. *Journal of Fluid Mechanics*, 93(01): 185–207, 1979.

[13] H. Wong. A Brief Overview on some Resonance Phenomena in Nozzle Flows, AIAA 2004-4013. In *40th AIAA/ASME/SAE/ASEE Joint Propulsion Conference and Exhibit, 11 - 14 July 2004, Fort Lauderdale, Florida*, 2004.

[14] M. Frey. *Behandlung von Strömungsproblemen in Raketendüsen bei Überexpansion*. PhD thesis, Universität Stuttgart, Holzgartenstr. 16, 70174 Stuttgart, 2001. URL http://elib.uni-stuttgart.de/opus/volltexte/2001/800.

[15] S. Deck and P. Thorigny. Unsteadiness of an Axisymmetric Separating-Reattaching Flow: Numerical Investigation. *Physics of Fluids*, 19(6):065103, 2007.

[16] D. Saile. TRP on Hot Plume Testing Facilities for ELV Propulsion Characterization, WP2100: Scope of Operation of Wind Tunnel. *Ref.: Proposal-No. 3005921*, 2013.

[17] D. Deprés. *Analyse Physique et Modélisation des Instationnarités dans les Écoulements d'Arrière-Corps Transoniques*. PhD thesis, Université de la Méditerranée Aix-Marseille II, 2003.

[18] P.-E. Weiss, S. Deck, J.-C.Robinet, and P. Sagaut. On the Dynamics of Axisymmetric Turbulent Separating/Reattaching Flows. *Physics of Fluids*, 21(7): 075103, 2009.

[19] G.P. Sutton and O. Biblarz. *Rocket Propulsion Rlements, 7th ed.* John Wiley & Sons, 2010.

[20] D. Deprés, P. Reijasse, and J.P. Dussauge. Analysis of Unsteadiness in Afterbody Transonic Flows. *AIAA journal*, 42(12):2541–2550, 2004.

[21] V. Zapryagaev, A.V. Lokotko, S.V. Nikiforov, A.A. Pavlov, A.V. Tchernyshev, W.J. Bannink, H. Ottens, and J. Muylaert. Experimental Investigation of Base Pressure with Hot Supersonic Jet for External Supersonic Flow. In *Fourth Symposium on Aerothermodynamics for Space Vehicles*, volume 487, page 579, 2002.

[22] B.H. Goethert. Base Heating Problems of Missiles and Space Vehicles. *ARS Paper*, pages 1666–61, 1961.

[23] F.S. Simmons. *Rocket Exhaust Plume Phenomenology*. Aerospace Press El Segundo, CA, 2000.

[24] S. M. Dash. Rocket motor plume flowfields: Phenomenology and Simulation. In *In AGARD, Rocket Motor Plume Technology, ARARD-LS-188, ISBN 92-835-0713-4*, volume 1, 1993.

[25] J.S. Draper. Plume Separated Region as a Flameholder. *AIAA Journal*, 14(3):358–362, 1976.

[26] K. Kinefuchi, K. Okita, I. Funaki, and T. Abe. Prediction of In-flight Radio Frequency Attenuation by a Rocket Plume by Applying CFD/FDTD Coupling. *49th AIAA/ASME/SAE/ASEE Joint Propulsion Conference, July 14 - 17, 2013, San Jose, CA, AIAA 2013-3790*, 2013.

[27] NASA. NASA Thermal Infrared Camperas Capture SpaceX Falcon 9 First Stage Re-entry, Sept. 21, 2014, 2014. URL https://www.youtube.com/watch?v=riU3DZmU-jE.

[28] Unitary Plan Wind Tunnel NASA Langley. Entry, Descent and Landing Project, Supersonic Retropropulsion Test, July 2010, 2010. URL https://www.youtube.com/watch?v=i-coJg_vgxI.

[29] W.M. Marshall, S. Pal, R.D. Woodward, and R.J. Santoro. Benchmark Wall Heat Flux Data for a GO2/GH2 Single Element Combustor. *AIAA Paper*, 3572:2005, 2005.

[30] P. Sibtosh, W. Marshall, R. Woodward, and R.J. Santoro. Test Case RCM-1: Penn State Preburner Combustor. In *3rd International Workshop Rocket Combustion Modeling, March 13-15, 2006, Vernon, France*, pages 1–9, 2006.

[31] Editor: S. Schlechtriem. Institute of Space Propulsion Lampoldshausen, Status Report 2011, 2011.

[32] C. Manfletti, J. Sender, and M. Oschwald. Theoretical and Experimental Discourse on Laser Ignition in Liquid Rocket Engines. 2009.

[33] O.J. Haidn and M. Habiballah. Research on High Pressure Cryogenic Combustion. *Aerospace Science and Technology*, 7(6):473 – 491, 2003. ISSN 1270-9638. doi: http://dx.doi.org/10.1016/S1270-9638(03)00052-X. URL http://www.sciencedirect.com/science/article/pii/S127096380300052X.

[34] S. Magniant and P. Vinet and R. Blasi and J.-P. Dutheil and Taiichi Motomura. Airbus Defence and Space LOX/Methane Propulsion Demonstrator, IAC-14.C4.5.1. In *65th International Astronautical Congress, Toronto, Canada*, 2014.

[35] G. Le Forestier, P. Danous, G. Dantu, A. Preuss, F. Grauer, and R. Strunz. First Firing Test Campaign of European Staged-Combustion Demonstration. In *3rd EUCASS conference, Versailles, 6th-9th July*, 2009.

[36] I.A. Klepikov, B.I. Katorgin, and V.K. Chvanov. The New Generation of Rocket Engines, Operating by Ecologically Safe Propellant "Liquid Oxygen and Liquefied Natural Gas (Methane)". *Acta Astronautica*, 41(4):209–217, 1997.

[37] C. Bonhomme, M. Theron, E. Louaas, A. Beaurain, and E.P. Seleznev. French/Russian Activities on LOx/LCH4 Area. In *57th Astronautical Congress (International). Valence, Spain*, 2006.

[38] J. Breteau, Th. Kachler, B. Vieille, R. Tontini, R. Strunz, and G. Dantu. FLPP European Next Generation Launcher Propulsion High Thrust Engine Demonstrator. In *3rd EUCASS Conference, Versailles, 6th-9th July*, 2009.

[39] Y. Letourneur, F. Leleu, D. Pinard, J. Krueger, and M. Balduccini. Status of next generation expendable launchers concepts within the flpp program. *Acta Astronautica*, 66(9):1404–1411, 2010.

[40] P. Caisso, A. Souchier, C. Rothmund, P. Alliot, C. Bonhomme, W. Zinner, R. Parsley, T. Neill, S. Forde, R. Starke, et al. A Liquid Propulsion Panorama. *Acta Astronautica*, 65(11):1723–1737, 2009.

[41] K.-H. Kim and D.-S. Ju. Development of CHASE-10 Liquid Rocket Engine Having 10tf Thrust Using LOX & LNG (Methane). *AIAA Paper*, 4907:2006, 2006.

[42] H. Tamura, F. Ono, A. Kumakawa, and N. Yatsuyanagi. LOX/Methane Staged Combustion Rocket Combustor Investigation. *Rep./AIAA*, 1987.

[43] B.H. Goethert and L.T. Barnes. Some Studies of the Flow Pattern at the Base of Missiles with Rocket Exhaust Jets. Technical report, DTIC Document, 1960.

[44] B.H. Goethert. Base Flow Characteristics of Missiles with Cluster-Rocket Exhausts. *Aerospace Engineering*, 20(3):28, 1961.

[45] M. Frey. TRP on Buffeting Reduction, WP3200: Feasibility Study for the Plume Simulation. *Doc. No. TP24-TN122/2009*, 1(1):19, 2009.

[46] S. Stephan and R. Radespiel and R. Müller-Eigner. Jet Simulation Facility using the Ludwieg Tube Principle. In *5th European Conference for Aeronautics and Space Sciences (EUCASS), Munich, Germany, 2013*, 2013.

[47] B. Stahl, H. Esch, and A. Gülhan. Experimental Investigation of Side Jet Interaction with a Supersonic Cross Flow. *Aerospace Science and Technology*, 12 (4):269 – 275, 2008. ISSN 1270-9638. doi: http://dx.doi.org/10.1016/j.ast.2007.01.009. URL `http://www.sciencedirect.com/science/article/pii/S1270963807001010`.

[48] Bernhard Stahl, Hans Emunds, and Ali Gülhan. Experimental Investigation of Hot and Cold Side Jet Interaction with a Supersonic Cross-Flow. *Aerospace Science and Technology*, 13(8):488 – 496, 2009. ISSN 1270-9638. doi: http://dx.doi.org/10.1016/j.ast.2009.08.002. URL `http://www.sciencedirect.com/science/article/pii/S1270963809000443`.

[49] A. Preci and A. Gülhan. Free Flight Investigation of Atmospheric Entry Capsules in Low Subsonic Flow. In *In Proceedings of AIAA Atmospheric Flight Mechanics Conference, 5-9 January 2015, Kissimmee, Florida*, 2015.

[50] A. Preci, A. Gülhan, E. Clopeau, P. Tran, L. Ferracina, and L. Marraffa. Experimental Investigation of Dynamic Characteristics for MarcoPolo-R ERC in Low Subsonic Flow Using the Free Flight Technique. In *to be presented at 8th European Symposium on Aerothermodynamics for Space Vehicles, 2-6 March 2015, Lisbon, Portugal*, 2015.

[51] H. Emunds and edited by A. Ferri H. Riedel. *Contribution of the Institute für Angewandte Gasdynamik of the DFVLR, Porz-Wahn, In: Improved Nozzle Testing Techniques in Transonic Flow: Report of a Study organized by the AGARD Propulsion and Energetics Panel with the Collaboration of the Fluid Dynamics Panel and including Papers and Discussions from the Special Session on this Topic held at the 35th Fluid Dynamics Panel Meeting in Rome, Italy, 4-10 Sept. 1974*. Number 208. North Atlantic Treaty Organization, Advisory Group for Aerospace Research and Development, 1975.

[52] P.K. Tucker, S. Menon, C.L. Merkle, J.C. Oefelein, and V. Yang. Validation of High-Fidelity CFD Simulations for Rocket Injector Design. *AIAA Paper*, 5226:2008, 2008.

[53] J. L. Herrin and J. C. Dutton. Supersonic Base Flow Experiments in the Near Wake of a Cylindrical Afterbody. *AIAA journal*, 32(1):77–83, 1994.

[54] C. J. Bourdon and J. C. Dutton. Planar Visualizations of Large-Scale Turbulent Structures in Axisymmetric Supersonic Separated Flows. *Physics of Fluids (1994-present)*, 11(1):201–213, 1999.

[55] H. Esch. *Die 0,6x0,6-m-Trisonische Meßstrecke der DFVLR in Köln-Porz (Stand 1986), DFVLR-Mitt. 86-21*. Wissenschaftliches Berichtswesen der DFVLR, ISSN 0176-7739, Postfach 906058, 5000 Köln 90, 1986.

[56] Trisonic Test Section Cologne (TMK), Supersonic and Hypersonic Technology Department. URL `http://www.dlr.de/as/en/desktopdefault.aspx/tabid-194/407_read-5447/`.

[57] P.E. Weiss and S. Deck. Numerical Investigation of the Robustness of an Axisymmetric Separating/Reattaching Flow to an External Perturbation Using ZDES. *Flow, turbulence and combustion*, 91 (3):697–715, 2013.

[58] A. Ponomarenko. RPA-Tool for Rocket Propulsion Analysis. In *Space Propulsion Conference*, 2014.

[59] S.J. Isakowitz, J.P. Hopkins, and J.B. Hopkins. *International Reference Guide to Space Launch Systems*. AIAA (American Institute of Aeronautics & Astronautics), 1999.

[60] M. Sodomann. TOSCA Program Abilities, Doc.No.: FF-SR 3000-0061-01, 1996.

[61] US NOAA and US Air Force. US Standard Atmosphere, 1976. Technical report, NOAA-S/T, 1976.

[62] D. Saile and D. Kirchheck and A. Gülhan and C. Serhan and V. Hannemann. Design of a GH2/GOX Combustion Chamber for the Hot Plume Interaction Experiments at DLR. In *8th European Symposium on Aerothermodynamics for Space Vehicles*, 2015.

[63] K. Hasegawa, K. Kusaka, A. Kumakawa, M. Sato, M. Tadano, and H. Takahashi. Laser ignition characteristics of GOX/GH2 and GOX/GCH4 propellants. In *Joint Propulsion Conference*, 2003.

[64] V. Schmidt, D. Klimenko, O. Haidn, M. Oschwald, A. Nicole, G. Ordonneau, and M. Habiballa. Theoretical Investigation and Modeling of the Ignition Transient of a Coaxial H2/O2-Injector. 2003.

[65] T. Gerhold, M. Galle, O. Friedrich, and J. Evans. Calculation of Complex Three Dimensional Configurations Employing the DLR-TAU-code. In *In Proceedings of the 35th Aerospace Sciences Meeting and Exhibit, number AIAA-1997-167, Reno, USA*, 1997.

[66] A. Mack and V. Hannemann. Validation of the Unstructured DLR-TAU-Code for Hypersonic Flows. In *In Proceedings of the 32nd AIAA Fluid Dynamics Conference and Exhibit, AIAA-2002-3111*, 2002.

[67] S. Gordon and B.J. McBride. Computer Program for Calculation of Complex Chemical Equilibrium Compositions and Applications I. Analysis. *NASA RP-1311-P1*, 1994.

[68] B.J. McBride and S. Gordon. Computer Program for Calculation of Complex Chemical Equilibrium Compositions and Applications II. User's Manual and Program Description. *NASA RP-1311-P2*, 1999.

[69] S.N.B. Murthy and J.R. Osborn. Base Flow Phenomena with and without Injection - Experimental Results, Theories, and Bibliography. *Aerodynamics of base combustion.(A 76-37230 18-02) New York, American Institute of Aeronautics and Astronautics, Inc.*, pages 7–210, 1976.

[70] O. Bos, O. de Bruijn, N.P. van Hinsberg, T.J.J. Lombaerts, P. Lucas, D.M. Luchtenburg, J.A.S. Witteveen, and K.G. van der Zee. Feasibililty Study of a Hot Plume Test Facility. 2002.

[71] B.H. Goethert. Transonic Wind Tunnel Testing. Technical report, DTIC Document, 1961.

[72] C. Willert, M. Fischer, J. Heinze, and M. Voges. TRP on Hot Plume Testing Facilities for ELV Propulsion Characterization, WP2300: Measurement Techniques. *Ref.: Proposal-No. 3005921*, 2013.

[73] L. Lange, J. Heinze, M. Schroll, C. Willert, and T. Behrendt. Combination of Planar Laser Optical Measurement Techniques for the Investigation of Pre-mixed Lean Combustion. 2012.

[74] U. Doll, M. Fischer, G. Stockhausen, and C.E. Willert. Fundamentals of Filtered Rayleigh Scattering. 2012.

[75] S.P. Kearney, S.J. Beresh, R.W. Schefer, and T.W. Grasser. Filtered Rayleigh Scattering Diagnostic for Multi-Parameter Thermal-Fluids Measurements: LDRD Final Report. *Sandia Report, SAND2004-0158*, 2004.